

PAPER • OPEN ACCESS

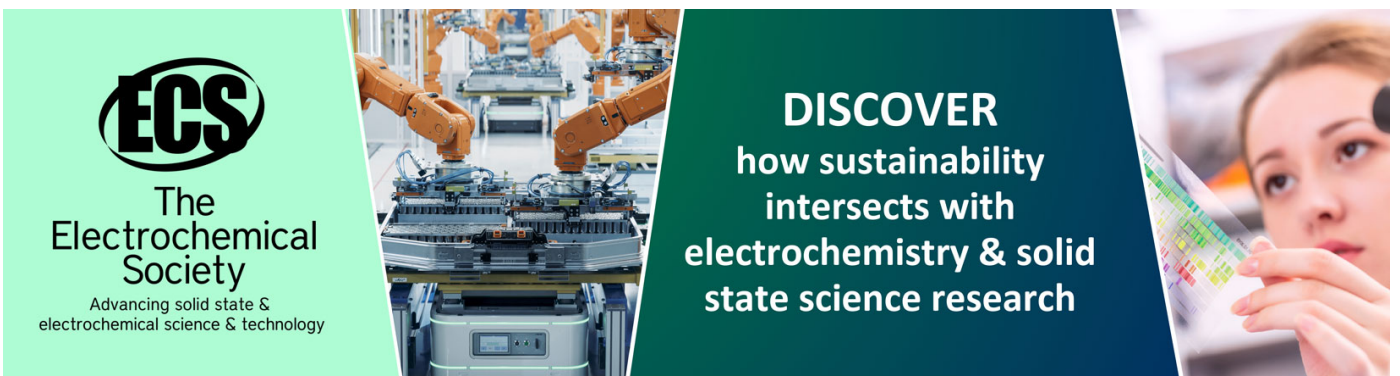
Strain distribution at the transition from bent to unbent regions in tube rotary draw bending: an in-situ, real-time measurement study

To cite this article: X He *et al* 2022 *IOP Conf. Ser.: Mater. Sci. Eng.* **1270** 012059

View the [article online](#) for updates and enhancements.

You may also like

- [Effect of heat treatment conditions on stamping deformation and springback of 6061 aluminum alloy sheets](#)
Guan Wang, Guangxu Zhu, Linyuan Kou et al.
- [Effect of Microstructure on the Instantaneous Springback and Time-dependent Springback of DP600 Dual Phase Steel](#)
Rongting Li, Ruimin Mai, Yongxi Jin et al.
- [Research Progress of Springback in Multi-Point Forming of Sheet Metal](#)
Xinqi Li and Shicheng Hu



ECS
The
Electrochemical
Society
Advancing solid state &
electrochemical science & technology

DISCOVER
how sustainability
intersects with
electrochemistry & solid
state science research

Strain distribution at the transition from bent to unbent regions in tube rotary draw bending: an in-situ, real-time measurement study

X He, J Ma and T Welo*

Department of Mechanical and Industrial Engineering, Norwegian University of Science and Technology, Trondheim, 7491, Norway

* Corresponding author, E-mail address: torgeir.welo@ntnu.no

Abstract. In tube bending processes, accurate control of springback is of crucial importance as this affects the dimensional accuracy of the final product and overall equipment efficiency. The distribution of stress and strain during bending is one of the most fundamental issues determining the springback magnitude of the product. In conventional analyses of rotary draw bending, the deformation behaviour along the bending direction is normally assumed to be uniform for constant-radius bends, following the contour of the die configuration. In practice, however, the stress-strain distribution is non-uniform, particularly at the transition between the bent and unbent regions of the formed component. The distribution makes a significant contribution to springback and its variations, especially for low bend-angle components. This research focuses on exploring the strain distribution at the end transition of the bend of aluminium tubes in rotary draw bending. An experimental test setup for strain measurements with a strain gauge glued to the unbent area has been designed and conducted to measure the strain distribution during bending. The characteristics of non-uniform strain distribution during tube bending, including the evolving transition behaviour at the transition between bent and unbent areas, are studied. The results enhance the understanding of deformation characteristics of bent tubes, and contribute to improved physically-based models and springback control routines in industrial practice.

1. Introduction

Bent tubular components are widely used in many industries such as aviation, automotive and offshore areas. Upon bending, various phenomena such as wrinkling, springback and cross-sectional distortion can occur, and seriously reduce the dimensional accuracy and the performance of formed products [1]. Strain distribution and its evolution—the most fundamental mechanism in metal forming—significantly influence the occurrence of many defects as well as their severity with regard to product quality and productivity during tube bending processes. Thus, establishing an in-depth understanding of the strain distribution and its evolution is of critical importance to control the process and improve the product quality of bent products.

Up to now, a significant number of works have been carried out to investigate the strain distribution in bending-based manufacturing processes. Examples may be given as Li et al. [2], who studied the axial strain distribution of the cross-section in the bent area by considering the effect of neutral layer shifting. Based on this Ma et al. [3] developed an analytical springback model which was used to explore the influence of axial strain distribution across the section on springback. Engel et al. [4] compared FE simulation with the analytically calculated neutral axis shifting, wall thickness changes as well as strain distribution in tube rotary draw bending. The results show that the shifting displacement of the neutral axis increases with increased bending angle, and the overall strain magnitude of the aluminium tube is



larger than that of the stainless-steel tube under the same bending condition. In addition, several studies used a localized differential heating method to reconstruct the shifting of the neutral layer and change the distribution of axial strain across the tube section, primarily to improve the bendability of hard-to-deform materials [5, 6].

However, the vast majority of the above studies focus on the strain distribution in the, in theory, bent area of tubular parts. Very few studies explore the strain transition from the bent to the unbent portions. Li et al. [7] measured the tangent and thickness strain distributions in tube bending via the etched grid method, finding that there is also a large level of strain at the tangent point, i.e. at the theoretical transition point. E et al. [8] found that the wall thickness change mainly occurs in the bent area and tends to gradually decrease from the bent portion to the unbent portion. Welo [9] proposed a steering model for closed-loop feedback springback prediction, in which the strain transition portion included a gradually decreasing bending moments over a certain distance in the pressure die region, in order to improve the accuracy of the springback control model. In his work, however, the strain distribution in the transition area is based on theoretical assumptions, and not experimentally measured results. However, the above attempts have definitely improved the understanding of strain distribution in the transition region between bent and unbent portions in tube rotary draw bending. At present, no studies can be found aiming to quantify the strain distribution at the transition region to the bent portion of the tube. In particular, the understanding of how the strain shifts from levels in the uniformly bent region, and over which distance the strains vanish in the transition area, remain unclear up to this point. Closing this identified knowledge gap will affect the analysis accuracy of the process. Taking the accuracy of springback upon unloading as an example, it is currently a limitation of the implementation of Industry 4.0 strategies and realization of zero-defect manufacturing in tube forming processes.

This paper experimentally studies the strain distribution evolution at the transition from bent to unbent regions. For this purpose, an in-situ measurement method for detection of real-time strain evolution along the bending process was developed. Moreover, a series of carefully controlled rotary draw bending experiments was conducted, using thin-walled AA6082-T4 tubes, as to be presented in Section 2. Based on the in-situ strain measurements, the strain distribution in the bent-unbent transition region will be quantitatively assessed in Section 3. Finally, the conclusions and outlook for future work are given in Section 4.

2. Method and experiments

2.1. Rotary draw bending (RDB)

A CNC rotary tube draw bending machine is used in the experiments in this paper. As one of the most widely used processes for bending tubes, RDB has the advantages of providing a large bending angle, tight bend radius and high flexibility that will ultimately result in low cost. The tube bending machine and dies used in this study are shown in figure 1. The tube is bent with a bend die that determines the bend radius of the formed tube. The clamp die has the same length as the grip area of the bend die. It holds the tube in position during bending and prevents slipping to take place. The pressure die contacts the tube from the initial position of bending and moves parallel with the unbent tube. In the study, the radius of the bend die is 222 mm; AA6082 tubes are used in the experiments, which are manufactured by extrusion process and naturally aged to stable T4 temper condition. The outer diameter (D) is 60 mm and the nominal wall thickness (t) is 2 mm.

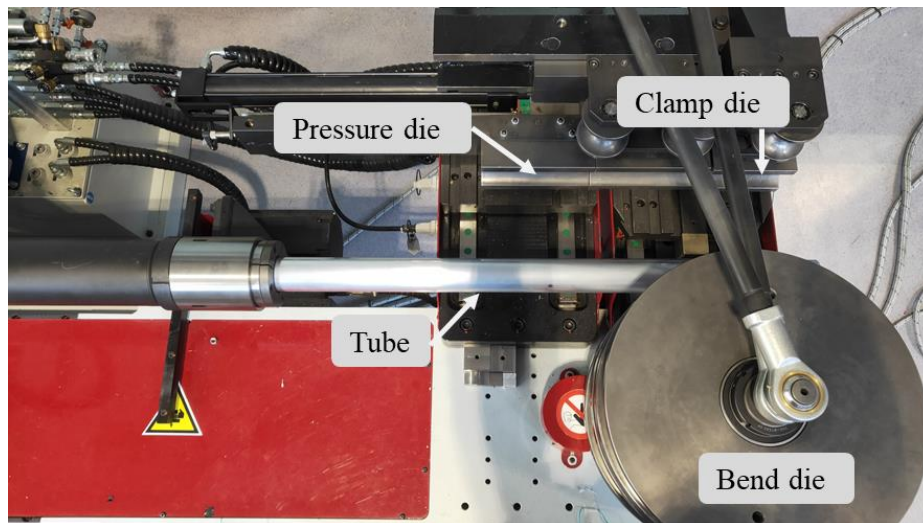


Figure 1. RDB machine and dies.

To determine an appropriate measuring method, including the capabilities of strain gauges, the maximum strain needs to be estimated. Assuming a pure bending condition where the neutral layer (NL) remains at the central line of the tube, the maximum nominal strain in the tangential direction at the extrados of the bent tube can be calculated by:

$$\varepsilon_m = \frac{y}{R_n} = \frac{\frac{d-t}{2}}{R_D} \approx 0.126 \quad (1)$$

where ε_m is the maximum tangential strain at the extremities, R_n is the radius of NL, R_D is the radius of the bend die.

2.2. Measuring method

Strain gauge sensors that can convert the change of dimension into electrical signals are commonly used for static or dynamic strain analysis. The change in resistance, which reflects the strain of the target material, can be measured and converted into an electrical signal. According to equation (1), the strain on the extrados of the bent area is around 12.6% under the pure bending assumption. Considering that the actual strain is not uniformly distributed in the bent-unbent transition area, the magnitude of strain around the tangent point should be below this theoretical value. Based on this, HBM 1-LD20-6/120 strain gauges with a maximum elongation of $\pm 100,000 \mu\text{m/m}$ ($\pm 10\%$) were used to measure the real-time strain in the area of interest during bending. The gauge has a resistance of 120Ω , and the length a and the width b of the measuring grid are 6 mm and 2.8 mm, respectively; the nominal value of the gauge factor is 2.07.

For this type of strain gauge, the change of resistance is measured through a Wheatstone bridge with one unknown resistance R_x and three known resistances R_1 , R_2 and R_3 . Consequently, R_x can be measured by balancing two legs of a bridge circuit at any point of time. In this paper, a quarter bridge was used where V_e is the excitation voltage and V_m is used to calculate the resistance changes of the strain gauge. Then, the strain of the measured region ε can be obtained:

$$\frac{V_m}{V_e} + \frac{R_3}{R_1+R_3} - \frac{R_x}{R_2+R_x} = \frac{R_x F_G}{R_2+R_x} \cdot \varepsilon \quad (2)$$

where the gauge factor F_G is the proportion of the percentage changes in resistance $\Delta R / R$ and the percentage changes in wire length $\Delta L / L$. Therefore, the strain is proportional to the ratio of measured voltage and excitation voltage when the four resistors have the same resistance.

2.3. Experimental procedure

In the rotary draw bending process, since the outside surface of the tube is in contact with the pressure die, the strain gauge is installed on the inside surface in the extrados of the tube and placed at the tangent

point (theoretical transition point between the bent and unbent regions). Figure 2 illustrates the measurement position and the sensor glued on the inside surface. Prior to gluing the surface around the target material was sanded with 500-grit sandpaper and cleaned with an ethanol solvent. The gauge was then bonded with a cyanoacrylate-based adhesive and cured for approximately 40 hours. Each lead of the strain gauge is soldered with a 2-meter wire, connected to a quarter bridge adapter that plugs into a channel of universal amplifier HBM Quantum X MX840B. It measures the resistance changes in the Wheatstone bridge circuit with a data acquisition frequency of 300 Hz.

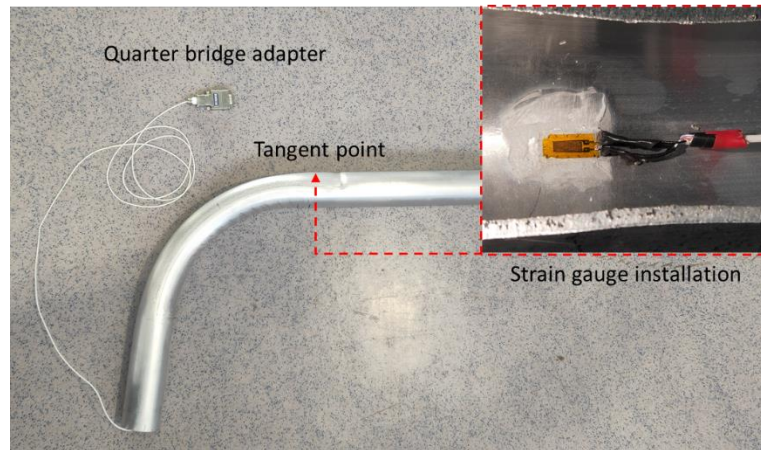


Figure 2. Strain gauge installation on the inner surface.

Figure 3 schematically illustrates the in-situ, real-time strain measurement process used in rotary draw bending. When the bending operation starts, the tubular material is fed towards the tangent point. At the same time, the strain gauge moves towards the tangent point together with the unbent tube. As a result, the recorded strain gradually increases while moving closer to the bent regions. Assuming that the strain distribution on the unbent portion of the tube remains constant during bending, the strain evolution with time can reflect the strain distribution in this area. Therefore, the strain distribution can be calculated from the velocity at the measurement point and a time-dependent evolution of the strain in the measurement area $S(t)$. The nominal velocity of the movement of the point is:

$$V_t = \frac{R_D \cdot \theta}{t_e - t_s} \quad (3)$$

where θ is the bending angle, t_s and t_e are the start and end time during bending, respectively. Then, the strain distribution in the unbent region is:

$$f(x) = [(t - t_s) \cdot V_t - R_D \cdot \theta, S(t)] = \left[R_D \theta \cdot \frac{t - t_e}{t_e - t_s}, S(t) \right] \quad (4)$$

Considering the strain is installed at the inner surface of the tube, the theoretical extrapolated strain of the extreme surface of tube extrados $f'(x)$ is:

$$f'(x) = \left[R_D \theta \cdot \frac{t - t_e}{t_e - t_s}, \frac{S(t) \cdot D}{D - t} \right] \quad (5)$$

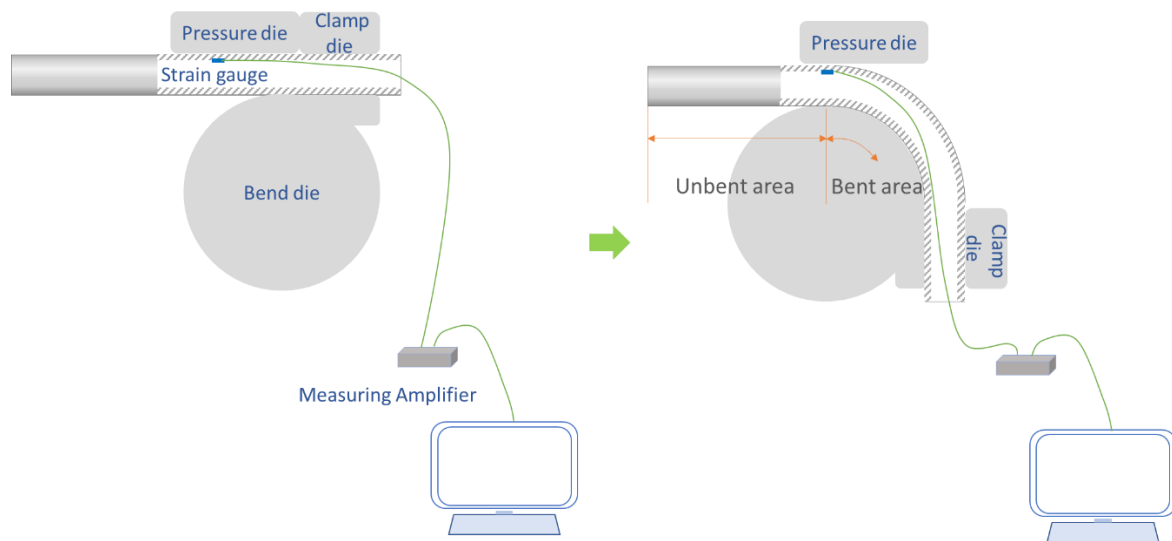


Figure 3. Schematic view of in-situ, real-time strain measurement method in tube rotary draw bending.

3. Result and discussion

3.1. Strain evolution with loading time

In the bending experiments, the measured strain changes accordingly with the relative position of the areas of interest (the strain gauge measurement areas) to the tangent point of the bend die. Based on bending experiments with different locations of strain gauge measurement, the strain evolutions of the measured areas with respect to the loading time are obtained and illustrated in figure 4. Here the actual angular velocity is about $4.8^\circ/\text{s}$ and the velocity of pressure die is about 18.4 mm/s . It is noted that the actual angular speeds mentioned above are the average values, and the effect of acceleration and deceleration at the beginning and the end of the bending operation are neglected.

As shown in figure 4, the strain evolution with time at the tangent point and the positions around 10 mm before and after are shown as blue, orange and grey lines, respectively. The strain evolutions throughout the bending process are re-processed to allow them to start at the same time (0 seconds) for a clearer comparison. Then, the three areas of interest enter a large strain state successively at 17 seconds. The bending operation is completed at 21 seconds, before releasing the clamp die after 26 seconds, resulting in an elastic driven strain relaxation of approximately 0.027%, 0.028% and 0.021%, respectively, for the three curves. The strain remains constant at the same level without further relaxation after unloading. As shown in figure 4, the overall increasing rates of three strain evolution curves present a similar trend with time. The strains increase gradually at the beginning, followed by an abrupt increase in the strain rate, after which the strain maintains a rapid increase until the end of bending. It can be found that the strain of the three curves shows a 0.5 to 1 second's difference in the time phase as they start bending at different times. The area at the tangent point remained at 4.81% strain before unloading, while the area around 10 mm in front of it has a strain of 2.92% and the area around 10 mm behind it is at 6.74%. This means that the strain distribution persists beyond the tangent point, representing the theoretical end-point for the bent component. This distribution will influence the dimensional springback characteristics of the tube, such as realized bend angle between two ends of the tube.

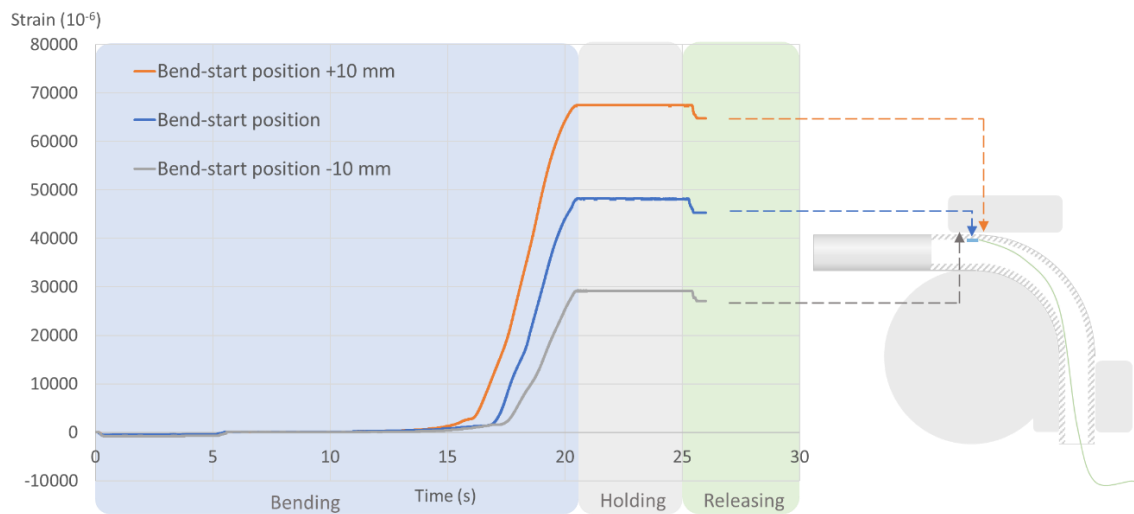


Figure 4. Measured strain evolutions during the tube rotary draw bending process.

In general, the tube reference points at different locations experience similar strain changes as they move towards the tangent point of the bend die. This may imply that with the increase of the bend angle, the variation of the strain distribution around the tangent point of the bend die is minor. In this study, such a potential variation is ignored, assuming that the strain distribution with respect to the tangent point of bend die in the transition region is stable. This gives a basis for converting the in-situ measured time-dependent strain evolution to the strain distribution in the transition area of the formed tube, as described in section 2.3.

3.2. Strain distribution at unbent area

Based on the in-situ measured time-dependent evolution of strains, the strain distribution in the transition area from bent to unbent regions can be calculated by equations (4) and (5). Taking the bending angle of 90° strain at the tangent point as an example, the start and end bending time were measured to be 0s and 18.6s, respectively. The distribution can be calculated and the approximate strain distribution on the unbent tube are shown in figure 5.

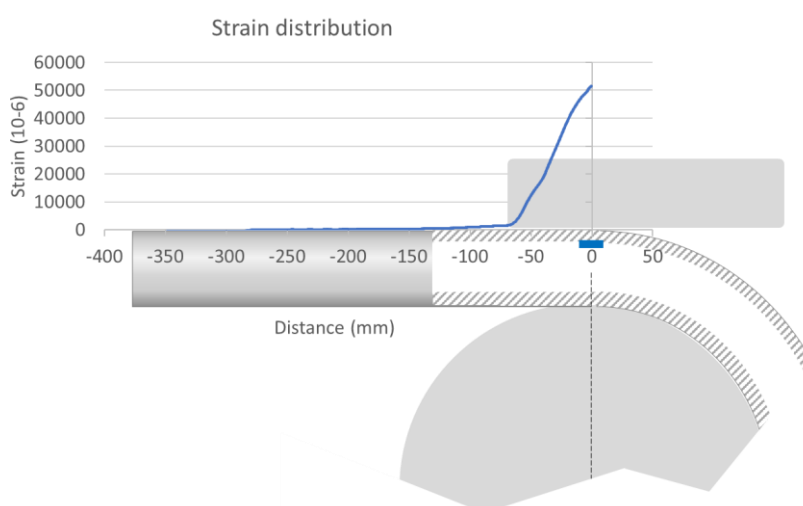


Figure 5. Calculated strain distribution at unbent area.

The strain larger than 0.1% is distributed within the region around 100 mm from the theoretical tangent point. Over this area, the strain experiences a rapid increase from the distance -70 mm to -60 mm and then increases almost linearly before it approaches the bent area. The pressure die covers an unbent region of the tube approximately 65 mm in front of the theoretical tangent point, which may be the

reason for the rapid increase in strain from the contacting area. Compared with the theoretical strain of 13% under a pure bending condition, the measured strain reaches around 5.2% at the boundary of the bent and unbent areas. The strain seems to increase to 7.2% according to the experiment at around 10 mm after the tangent point, while the strain after this position is not measured in this study due to the limitation of the capabilities of the strain gauge.

The research on springback control in rotary draw bending usually only considers the strain distribution in the normal bent region of the tube. In this study, however, the strain distribution extends 70 mm into the ‘unbent’ area, which will contribute to, for example, the realized bend angle. Thus, this gives a more comprehensive knowledge of bending behaviour and provides a basis for improved springback prediction.

3.3. Error analysis

Errors could be introduced due to the limitation of the measuring method in the experiments:

- “Average effect” of strain gauge. Since the centre of the strain gauge is used to represent the strain among the regions of $6 \times 2.8 \text{ mm}^2$, a maximum error of 3 mm may be introduced when the nonlinear strain gradient is large along the tube extrados.
- Positioning of strain gauge installation. Strain gauges are manually installed inside the tube, which may introduce minor position errors in the gauges.
- Acceleration and deceleration of bending speed. The process of acceleration and deceleration prolongs the time of bending, which could impact the calculated strain distribution.

4. Conclusion and future work

This paper presents an experimental investigation on the strain distribution and evolution at the transition between the bent and unbent regions in rotary draw bending, using an in-situ, real-time measurement method. The real-time strain evolutions at the positions around the bending tangent point were measured during the entire forming process, and further converted to the strain distribution in the bent-unbent transition area of the formed tube. This paper fills some of the research gap related to understanding the strain transition behaviour in the unbent region: the rapid shift of strain from the bent to unbent region; the magnitude of strain around the boundary of bent and unbent regions and the length of strain distribution region in the unbent portion of the tube in an RDB case study. The founding could potentially help to further improve the control of dimensional accuracy of the tube bending process, for instance, taking into account the strain transition in the unbent portion and the length of the strained region when calculating the springback of the tube in bend process.

However, the in-situ measurement of strain distribution presented herein is placed on the extrados in the pressure die area. To get a more in-depth understanding of the strain transition behaviour, in-situ measurement needs to be extended to the area of the intrados and the clamping areas. Furthermore, the influence of strain transition on the analysis of process behaviour in tube bending—in particular the springback prediction—will be studied to develop models for the control of forming process and the improvement of product quality.

References

- [1] Yang H, Li H, Zhang Z, Zhan M, Liu J and Li G 2012 Advances and trends on tube bending forming technologies. *Chinese J. Aeronaut.* **25** 1-12
- [2] Li H, Ma J, Liu B, Gu R and Li G 2018 An insight into neutral layer shifting in tube bending. *Int. J. Mach. Tool. Manu.* **126** 51-70
- [3] Ma J, Li H and Fu MW 2021 Modelling of springback in tube bending: A generalized analytical approach. *Int. J. Mech. Sci.*, **204**
- [4] Engel B and Hassan HR 2014 Investigation of neutral axis shifting in rotary draw bending processes for tubes. *Steel Res. Int.* **85** 1209-14
- [5] Ghiotti A, Simonetto E and Bruschi S 2021 Insights on tube rotary draw bending with superimposed localized thermal field. *Cirp. J. Manuf. Sci. Tec.* **33** 30-41

- [6] Yang H, Li H, Ma J, Li G and Huang D 2021 Breaking bending limit of difficult-to-form titanium tubes by differential heating-based reconstruction of neutral layer shifting. *Int. J. Mach. Tool. Manu.* **166**
- [7] Li H, Yang H and Shi KP 2012 Study on 3D strain distribution characteristics using etched grid method in tube bending. *Appl. Mech. Mater.* **184-185** 505-9
- [8] E DX, Chen JS, Ding J and Bai X 2012 In-plane strain solution of stress and defects of tube bending with exponential hardening law. *Mech. Based Des. Struc.* **40** 257-76
- [9] Welo T 2013 Intelligent manufacturing systems: Controlling elastic springback in bending. *IFIP Adv. Inf. Comm. Te.* **397** 460-6

Acknowledgement

This project was funded by Department of Mechanical and Industrial Engineering at Norwegian University of Science and Technology (NTNU), NTNU Aluminium Product Innovation Centre (NAPIC), and the TaFF project (Digitally-Controlled, Toolless and Flexible Forming, project No.: 317777) sponsored by Research Council of Norway.